CrossMark

ORIGINAL ARTICLE

Analysis of the variation in low-level laser energy density on the crushed sciatic nerves of rats: a morphological, quantitative, and morphometric study

Eduardo Keiske Mastuda Ziago[1] · Valéria Paula Sassoli Fazan[2] ·
Mamie Mizusaki Iyomasa[1] · Luiz Gustavo Sousa[1] · Paula Yumi Yamauchi[1] ·
Eunice Aparecida da Silva[2] · Eduardo Borie[3] · Ramón Fuentes[3] · Fernando José Dias[2,3]

Abstract The objective of this study was to evaluate three energy densities of low-level laser therapy (LLLT, GaAlAs, 780 nm, 40 mW, 0.04 cm^2) for the treatment of lesions to peripheral nerves using the sciatic nerve of rats injured via crushing model (15 kgf, 5.2 MPa). Thirty Wistar rats ($\male$, 200–250 g) were divided into five groups ($n = 6$): C—control, not injured, and irradiated; L0—injured nerve without irradiation; L4—injured nerve irradiated with LLLT 4 J/cm^2 (0.16 J); L10—injured nerve irradiated with LLLT 10 J/cm^2 (0.4 J); and L50—injured nerve irradiated with LLLT 50 J/cm^2 (2 J). The animals were sacrificed 2 weeks after the injury via perfusion with glutaraldehyde (2.5%, 0.1 M sodium cacodylate buffer). The nerve tissue was embedded in historesin, cut (3 μm), mounted on slides, and stained (Sudan black and neutral red). The morphological and quantitative analysis (myelin and blood capillary densities) and morphometric parameters (maximum and minimum diameters of nerve fibers, axon diameter, G-ratio, myelin sheath thickness) were assessed using the ImageJ software. ANOVA (parametric) or Kruskal-Wallis (nonparametric) tests were used for the statistical analysis. Groups L0, L4, L10, and L50 exhibited diminished values of all the quantitative and morphometric parameters in comparison to the control group. The morphological, quantitative, and morphometric data revealed improvement after injury in groups L4, L10, and L50 (irradiated groups) compared to the injured-only group (L0); the best results, in general, were observed for the L10 group after 15 days of nerve injury.

Keywords Nerve regeneration · Low-level laser therapy · Energy density · Morphology and morphometry

Introduction

Peripheral nerves are composed of neuron extensions, glial cells, and connective tissue; their peripheral portions are dependent on the continuity and integrity of the central portion [1–3]. The peripheral nerve injuries occur more often than spinal cord lesions [3, 4], 30% of which arise from lacerations due to sharp objects and long bone fractures and the remaining due to penetrating injuries, crush, ischemia, traction, electric shock, and vibration [4].

Peripheral nerve injuries result in a loss or reduction of sensation and motor activity of the innervated area. The injuries usually lead to retrograde axonal degeneration of neurons in the spinal cord, followed by slow and often incomplete regeneration [5]. Nerve crush injury is a common type of nerve damage that results in experimentally induced axonal interruption but preserves the conjunctive sheaths, called axonotmesis [6].

The regeneration of peripheral nerves must be accomplished via multiple approaches in addition to surgical options, such as incorporating low-level laser therapy (LLLT) [3, 7]. The precise photobiomodulation mechanisms of near-infrared (NIR) light and their therapeutic benefits have not been fully understood. NIR light (600–1200 nm) has

✉ Fernando José Dias
  fernando.dias@ufrontera.cl

[1] School of Dentistry, University of São Paulo, USP, Ribeirão Preto, Brazil

[2] School of Medicine, University of São Paulo, USP, Ribeirão Preto, Brazil

[3] Department of Integral Dentistry, CICO – Research Centre in Dental Sciences, Dental School, Universidad de La Frontera, Temuco, Chile

 Springer

significant photobiomodulation capacity, whereby their photons are absorbed by cytochrome C oxidase in the mitochondrial respiratory chain, which is the initial trigger of photobiomodulation. The increased activity of cytochrome C oxidase in turn increases the production of adenosine triphosphate (ATP), which in wounds or areas with low blood perfusion can activate injured cells and metabolic disorders [8].

Many studies have shown the importance of photobiomodulation therapy in neurology for the treatment of stroke, traumatic brain injury, brain degenerative disease, spinal cord injury, and peripheral nerve regeneration [9]. The photochemical and photobiological effects of LLLT at the cellular level can induce trophic conditions and inhibit inflammatory processes, which are necessary for nerve regeneration [10]. LLLT improves neurite outgrowth, ATP production, gene expression, and secretion of neural factors [11].

However, there is a wide variation among the physical parameters used in the application of the laser on nerve lesions, particularly regarding the energy density. In animal studies, for crushed or sectioned peripheral nerves of posterior paws (hindlimb), the studied energy densities ranged from 3 to 80 J/cm^2, passing through 4, 5, 8, 10, 15, 20, 40, 50, and 60 J/cm^2 [12–22]. Most studies revealed some functional and/or morphological improvement [12, 14, 15, 17, 19, 20]. However, improvements were not observed in some studies [13, 18].

The incidence of peripheral nerve injuries is still high, and still there are no fully effective treatments for recovery from these injuries, which causes a loss in the quality of life. Current studies have revealed many promising results for the use of low-level lasers in the recovery of nerve damage, although significant variability in the physical parameters has also been observed in these studies. This study sought to better understand the treatment of peripheral nerve injuries by analyzing three power densities of photobiomodulation therapy with LLLT (4, 10, and 50 J/cm^2) often applied to nerve damage which revealed promising results previously, in order to compare objectively and directly changes and possible improvements of these three protocols of LLLT.

The hypothesis of this study is that different LLLT energy densities can generate different morphological and morphometric responses related to regeneration of the nerve injured by a controlled compression. We aimed to determine whether these three energy densities (4, 10, or 50 J/cm^2) reveal the most significant improvement in nerve structure.

Materials and methods

Animals

Thirty Wistar rats (male, 200–250 g), were allocated in five groups ($n = 6$) (Table 1). The animals were kept at in a

bioterium in polypropylene boxes (Beiramar Ltda, Santo Antonio, SP, Brazil) with four animals per cage. The housing environment was maintained at 22 to 24 °C with 12 h of daylight per 24 h and cycling air, and animals were given food and water ad libitum.

For nerve injury, animals were anesthetized with ketamine (75 mg/kg, Agener Uniao, São Paulo, Brazil) and xylazine (10 mg/kg, Hertape, Juatuba, MG, Brazil) followed by hair removal from the lateral face of the left hind paw. An incision, using no. 24 scalpel blade (EMBRAMAC, Campinas, SP, Brazil), in the skin and divulsion of the gluteus maximus and biceps femoris to the left sciatic nerve were exposed. The injury site was standardized based on the location of the upper and lower bone spines on the ventral face of the iliac crest. The skin incision (~2 cm) was perpendicular to the line joining these bony processes and down 2 cm caudally in the lateral hind paw.

The animals were placed over a stainless steel base constructed to induce nerve damage using a "dead weight." For the controlled crushing of the left sciatic nerve, a 15-kg load was applied to the sciatic nerve to induce lesion [23] for 10 min with a circular crush area ~0.2826 cm^2 (Ø 0.6 cm, 5.2 MPa, 53.07 kgf/cm^2) (Fig. 1a). After the injury, the sciatic nerve was repositioned, the skin was sutured using a nylon 4-0 suture, and 10 mg/ml of anti-inflammatory agent flunixin meglumine (Banamine, MDS, Cruzeiro, SP, Brazil) and the broad-spectrum antibiotic pentabiotic (Fort Dodge, Zoetis, Campinas, SP, Brazil) were administered.

Low-level laser application

The Twin Laser (MMO, São Carlos, SP, Brazil) (GaAlAs) device was used. Six irradiations were applied on 6 alternate days at three points of the injured nerve region, corresponding to the proximal, distal, and central regions of the lesion, based on the same anatomical locations used to perform injury of the sciatic nerve. The animals were mechanically restrained, preventing the need to use general anesthesia, and thus reducing the loss of animals during the application of LLLT (Fig. 1b). The irradiation parameter data are presented in Table 2.

Collection and processing of the material

After 2 weeks of nerve injury, the animals were killed via rupture of the diaphragm under general anesthetic followed by intra-cardiac perfusion with 0.05 M phosphate buffer (pH 7.4) for vascular cleaning and glutaraldehyde (2.5% in buffer sodium cacodylate, 0.1 M, pH 7.2, 1 ml/g, MERCK, Darmstadt, Germany) for fixation. Following dissection, the tissue was collected, processed, and embedded in historesin (Leica, Wetzlar,

Table 1 Experimental groups

Control group (C)	- Anesthetized animals and lateral position for 10 min
Laser group 0 (L0)	- Anesthesia and nerve compression (15 kgf, 10 min)
Laser group 4 (L4)	Anesthesia, nerve compression (15 kgf, 10 min), LLLT of 4 J/cm2 (Belchior et al. [12], Dos Reis et al. [13])
Laser group 10 (L10)	- Anesthesia, nerve compression (15 kgf, 10 min), LLLT of 10 J/cm^2 (Barbosa et al. [14])
Laser group 50 (L50)	- Anesthesia, nerve compression (15 kgf, 10 min), LLLT of 50 J/cm^2 (Medalha et al. [16])

Germany). The tissue was obtained from microtome cuts (3 μm) of the nerves followed by mounting on histological slides. To stain the slides, the slides were soaked in 100% alcohol (MERCK, Darmstadt, Germany) for 15 min, followed by successive baths in Sudan black (VETEC, Duque de Caxias, RJ, Brazil) for 15 min and neutral red for 2 min and washing in distilled water. We opted for this color because Sudan black stains the lipid portion [24] of the myelin sheaths, and the background is stained by neutral red (VETEC, Duque de Caxias, RJ, Brazil), improving image contrast.

Qualitative morphological analysis

The histological sections were stained with Sudan black and neutral red and photographed using a M2 Zeiss microscope with an AxioCam camera MRc (Zeiss, Oberkochen, Germany) and the images were digitally stored. The nerves
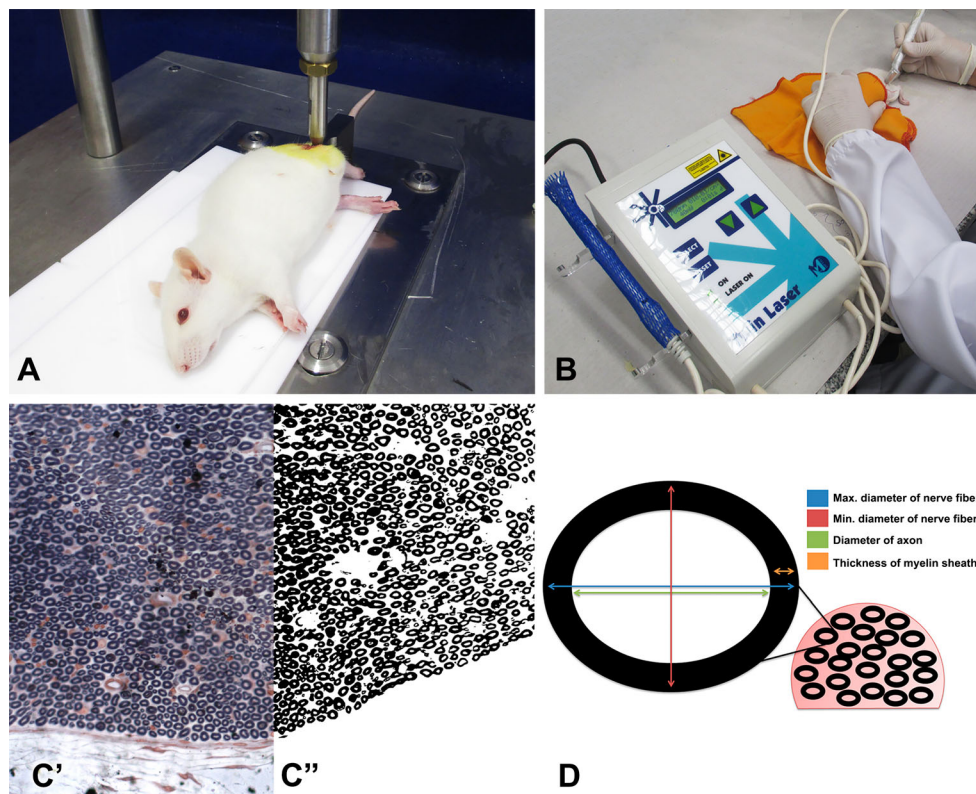

Fig. 1 Material and methods. *A* Sciatic nerve lesion by controlled compression model (15 kgf, 5.2 MPa, 10 min) using stainless steel apparatus especially made for this purpose. *B* Application of LLLT (Twin Laser MMOptics) using mechanical containment method. *C'* Preparation of histological images for the myelin quantification analysis. Original image obtained under the microscope (mag. ×320). *C"* Picture prepared for analysis using the ImageJ software showing binary (*black* and *white*) images, areas around the nerve, and deleted capillaries (mag. ×320). *D* Representative sketch of a nerve fiber that shows the morphometric parameters analyzed. *Blue arrow*—maximum diameter of nerve fiber. *Red arrow*—minimun diameter of nerve fiber. *Green arrow*—diameter of the axon. *Orange arrow*—thickness of the myelin. G-ratio—"diameter of the axon/maximum diameter of the nerve fiber"

Table 2 LLLT irradiation parameters

Power	40 mW (0.04 W)
Intensity	1 W/cm^2
Energy density	4, 10, and 50 J/cm^2
Wavelength	780 nm
Irradiation time (per point/total)	4/12, 10/30, and 50/150 s
Irradiations points number	3
Type	Continuous wave (CW)
Beam direction	Perpendicular to the skin
Deposited energy (per point/total)	0.16/0.48, 0.4/1.2, and 2/6 J
Spot irradiation area	0.04 cm^2
Number of sessions	6 (alternate days)

were analyzed and photographed. A comparative analysis of the morphological characteristics of the samples of the five study groups was then performed.

Quantitative histological analysis

The regions around the nerve, blood vessels, and areas of nerve degeneration were deleted such that the figures reported here do not include these areas as myelin sheaths. The images were processed in pure black and white (binary), and the dark area was quantified using the ImageJ software (National Institutes of Health NIH, Stapleton, NY, USA), yielding the area of myelin by quantifying the number of black pixels (Fig. 1(c') and (c'')). The total nerve area surrounding the nerve in the original image was obtained using the ImageJ software, and the final value obtained was the ratio of the area of myelin to nerve total area (area myelin/nerve area), which was compared among the groups. In addition, the capillaries present in the nerve were quantified and subsequently used to calculate capillary density, i.e., the number of capillaries present in the area of the nerve (capillaries/mm^2).

Morphometric analysis

The morphometric analyses were performed on the original images using the ImageJ software. The parameters evaluated were the maximum (blue arrow, Fig. 1d) and minimum diameters of nerve fiber (red arrow, Fig. 1d), which represent distinct values since usually the shape of the nerve fibers is represented by an ellipse; the diameter of the axon (green arrow, Fig. 1d); the G-ratio (ratio between the axon diameter and the nerve fiber diameter), which takes a value ranging from 0 to 1 corresponding to the degree of myelination of fibers [25–27]; and the thickness of the myelin sheaths (orange arrow, Fig. 1d). In each group, 18 photomicrographs, 3 per animal, were evaluated.

Statistical analysis

Statistical analysis was performed with using the SigmaPlot 12.0 software (Systat software Inc, San Jose, CA, USA). The Shapiro-Wilk test was selected to assess data normality. For data with normal distributions, the one-way ANOVA ($p = 0.05$) with the Holm-Sidak post hoc test [28] was employed, and the data are presented as the mean ± SD. For data that did not follow a normal distribution, we used the Kruskal-Wallis followed by a Dunn's post hoc test, in which case, the data are presented as the median, low (25%), and high (75%).

Results

Qualitative morphological analysis

The images reveal the different characteristics among the five protocols applied in the different study groups after 15 days of nerve injury.

The histological analysis revealed that the sciatic nerve crush lesion induced with a load of 15 kgf for 10 min was effective in destroying nerve fibers, as the injured groups (L0, L4, L10, and L50; Fig. 2b–i) showed a clear reduction in the number and size of nerve fibers compared to the control group (C; Fig. 2a).

The injured group that was not irradiated L0 (Fig. 2b, c) exhibited formation of glial cells, such as Schwann cells, which are important for the support and maintenance of nerve fibers. These cells occupied nearly the entire area of the transverse section and thus present in higher number than observed in the control group C, and fewer and smaller nerve fibers with thin myelin layers and a spaced distribution were noted in the L0 group.

The irradiated groups (L4, L10, and L50) showed an improvement in post-injury status compared to L0 beyond the critical period of 15 days, for which the results differed based on the applied energy density.

The L4 group with 4 J/cm^2 (Fig. 2d, e) showed an improvement in the morphological characteristics compared with the L0 group due to the greater amount of myelinated nerve fibers with larger diameters, although many Schwann cells were still observed in the myelin degeneration areas. The L4 results clearly revealed lower quality compared to the control group.

The energy densities of 10 and 50 J/cm^2 (L10, Fig. 2f, g and L50, Fig. 2h, i) improved the morphologies of the nerve fibers in comparison to L0 and L4. The myelin fibers were larger and more numerous and exhibited a more uniform distribution in the cross-sectional area of the sciatic nerve. The number of Schwann cells decreased, although these cells were still present, especially in the L50 group.
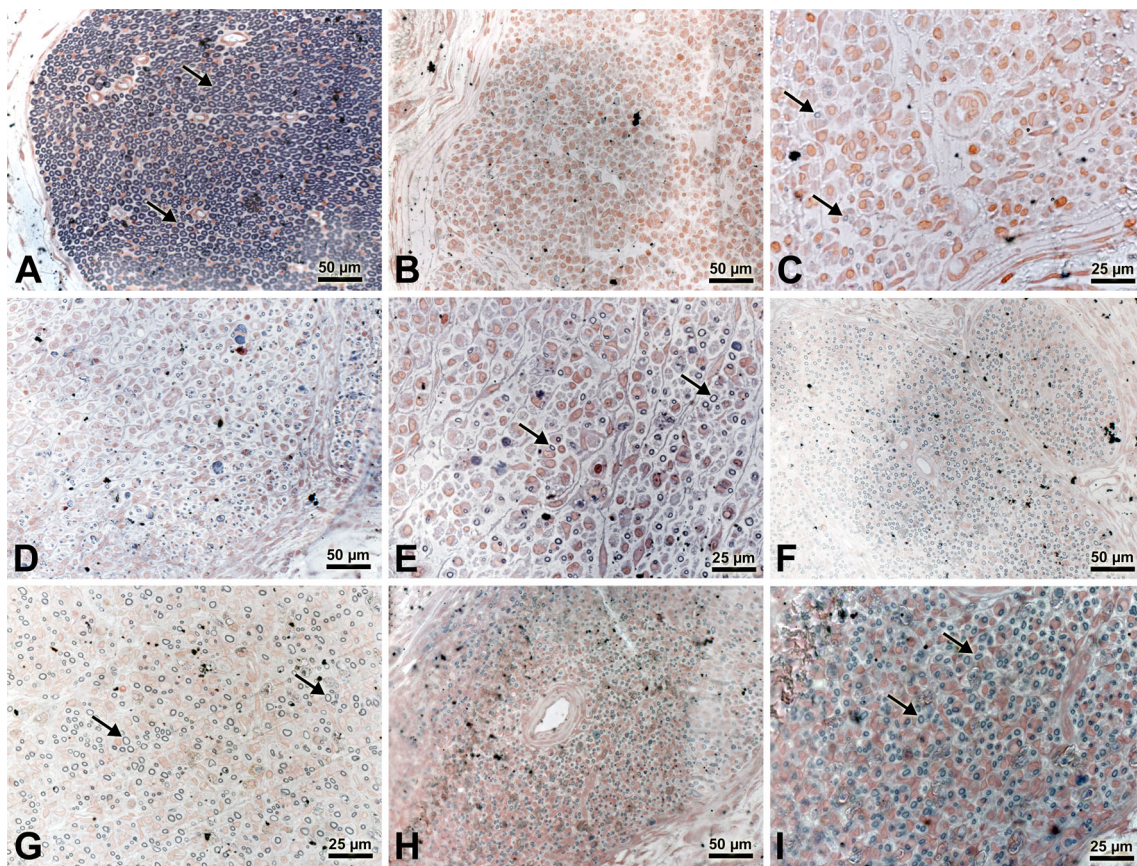
Fig. 2 Histological images. **a**–**c** Sciatic nerve with normal morphology showing nerve fibers (*arrow*), glial cells (*short arrow*), and capillaries (*arrowhead*) (mag. **a**, ×320; **b**, ×640). **c**, **d** L0 group—crushed sciatic nerve (15 kgf) without LLLT irradiation showing reduced nerve fibers (*arrow*), many glial cells (*short arrow*), and capillaries (*arrowhead*) (mag. **c**, ×320; **d**, ×640). **e**, **f** L4 group—crushed sciatic nerve (15 kgf) with LLLT irradiation of 4 J/cm², revealing nerve fibers (*arrow*), glial cells (*short arrow*), and capillaries (*arrowhead*) (mag. **e**, ×320; **f**, ×640). **g**, **h** L10 group—crushed sciatic nerve (15 kgf) with LLLT irradiation of 10 J/cm² showing nerve fibers (*arrow*), glial cells (*short arrow*), and capillaries (*arrowhead*) (mag. **g**, ×320; **h**, ×640). **i**, **j** L50 group—crushed sciatic nerve (15 kgf) with LLLT irradiation of 50 J/cm² showing nerve fibers (*arrow*), glial cells (*short arrow*), and capillaries (*arrowhead*) (mag. **i**, ×320; **j**, ×640)

Quantitative histological analysis

Myelin density

To analyze of the density of myelin, cross-sectional areas of the samples were subjected to an ANOVA on ranks test and Dunn's post hoc test due to failure of the Shapiro-Wilk normality test ($p = 0.03$). Group C (52.88, 47.89, and 61.19%) exhibited the highest value for this parameter, with a significant difference compared to the other study groups, L0 (8.84, 1.79, and 11.95%), L4 (13.54, 5.10, and 19.08%), L10 (12.43, 9.27, and 21.28%), and L50 (14.69, 6.33, and 18.56%) (Fig. 3a).

Capillary density

ANOVA and a Holm-Sidak post hoc test were used for the statistical analysis of the density of blood capillary because the data samples exhibited a normal distribution. The capillary density data revealed that the injured group without treatment L0 (54.25 ± 26.4 cap/mm²) showed a significant reduction in the number of vessels compared to the control group C (85.65 ± 22.64 cap/mm²). Among the treated groups, the L4 (73.0 ± 23.51 cap/mm²) group was the only group similar to L0; however, the L4 group was also similar to groups L50 (92.65 ± 37.47 cap/mm²) and C. The group with the largest capillary density was the L10 group (107.12 ± 33.07 cap/mm²), which was significantly different than the L0 and L4 groups and similar to the C and L50 groups (Fig. 3b).

Morphometric analysis

All morphometric data on the maximum and minimum diameters of the nerve fibers, axonal diameters, myelin thickness, and G-ratio were not normally distributed, and thus, for the statistical analyses, we used an ANOVA on ranks test followed by a Dunn's post-test. The data are presented as the median, 25 and 75%.
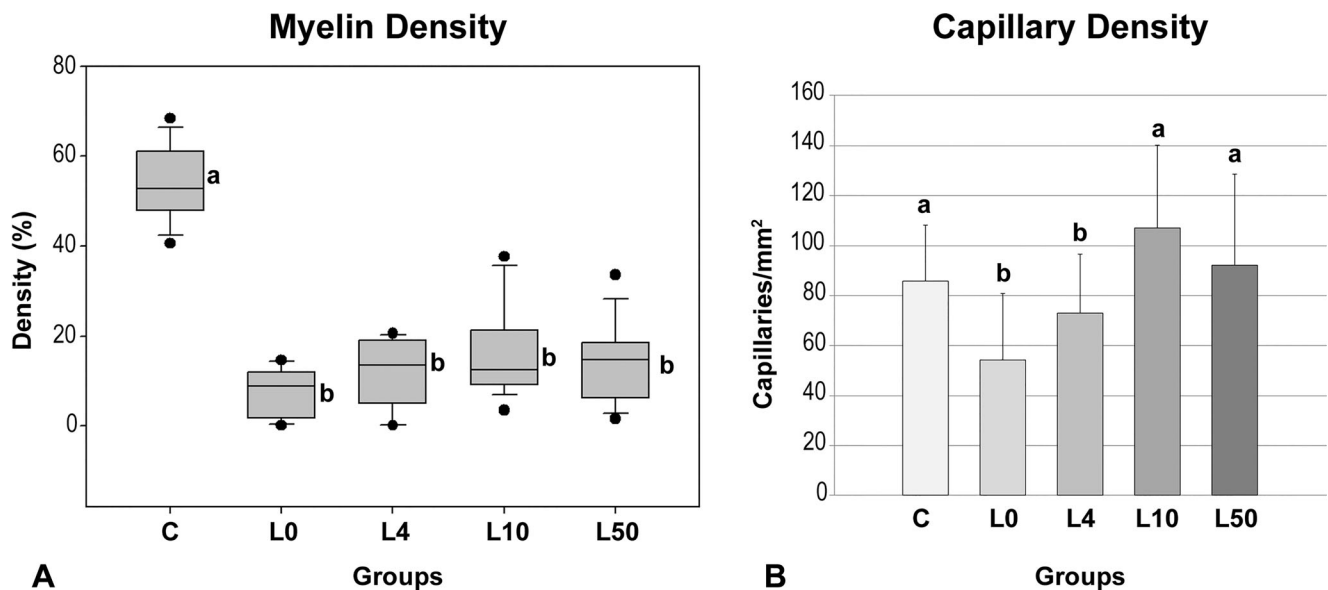
Myelin Density

Capillary Density

Fig. 3 Histological quantification. **A** Myelin density analysis graph (ratio between the area of the myelin nerve area of the cross section) for the six rats of the study groups; the *letters* represent significant differences ($p < 0.05$). **B** Graph of the densities of capillaries (number of capillaries/ nerve cross-section area in mm^2) for the six rats of the study groups; letters *a* and *b* represent significant differences ($p < 0.05$)

Maximum diameter of nerve fiber

Regarding the maximum diameter of the nerve fibers, all of the groups differed from one another, except the L4 (0.88, 0.71, and 1.16 μm) and L10 (0.91, 0.77, and 1.1 μm) groups, which were similar regarding the upper values of the median compared to the other injured groups. The control group (1.62, 1.45, and 1.81 μm) showed the highest values for the maximum diameter of the nerve fiber, and the L0 group (0.74, 0.6, and 0.88 μm) showed the lowest value for this parameter. The L50 group (0.85, 0.68, and 1.04 μm) had values between the C and L0 groups (Fig. 4a).

Minimum diameter of nerve fiber

The minimum diameter of nerve fiber differed among all groups, except the L4 (0.6, 0.49, 0.79 μm) and L50 (0.6, 0.49, and 0.74 μm) groups, which were similar. Group C (1.1, 0.96, and 1.26 μm) had the highest values, and the L0 group (0.74, 0.6, and 0.88 μm) had the lowest values for this morphometric parameter. Notably, the L10 group (0.65, 0.55, and 0.79 μm) exhibited values between the C and L0 groups, with slightly larger values than the medians of L4 and L50 groups (Fig. 4b).

Axonal diameter

The axonal diameter differed among all study groups, except between the groups L4 (0.52, 0.41, and 0.71 μm) and L50 (0.52, 0.41, and 0.66 μm), which were similar. The untreated

injured L0 group (0.41, 0.33, and 0.52 μm) exhibited the lowest values, and the control group C (0.88, 0.77, and 1.04 μm) had the highest values for this morphometric parameter. Among the groups irradiated with LLLT, the L10 group (0.58, 0.47, and 0.74 μm) had the highest median value (Fig. 4c).

Myelin thickness

The thickness of the myelin sheath of the nerve fibers was higher in the C group (0.37, 0.31, and 0.44 μm) compared to the other groups. The lowest values were observed for the L0 (0.15, 0.11, and 0.18 μm) and L50 (0.15, 0.12, and 0.2 μm) groups, which were similar to each other, followed by the L4 (0.18, 0.14, and 0.22 μm) and L10 (0.16, 0.12, and 0.20 μm) groups, which were also similar to each other that exhibited the highest median values compared to the other injured groups (Fig. 4d).

G-ratio

Regarding the G-ratio, a parameter that measures the degree of myelination of nerve fibers, the C group (0.55, 0.48, 0.60) had the lowest value, followed by the L0 (0, 58, 0.53, 0.65) and L4 (0.60, 0.53, 0.66) groups, which exhibited similar values with slightly larger median values. Finally, the highest G-ratio values were noted for the L10 (0.63, 0.57, 0.69) and L50 (0.62, 0.56, 0.68) groups, which were also similar (Fig. 4e).
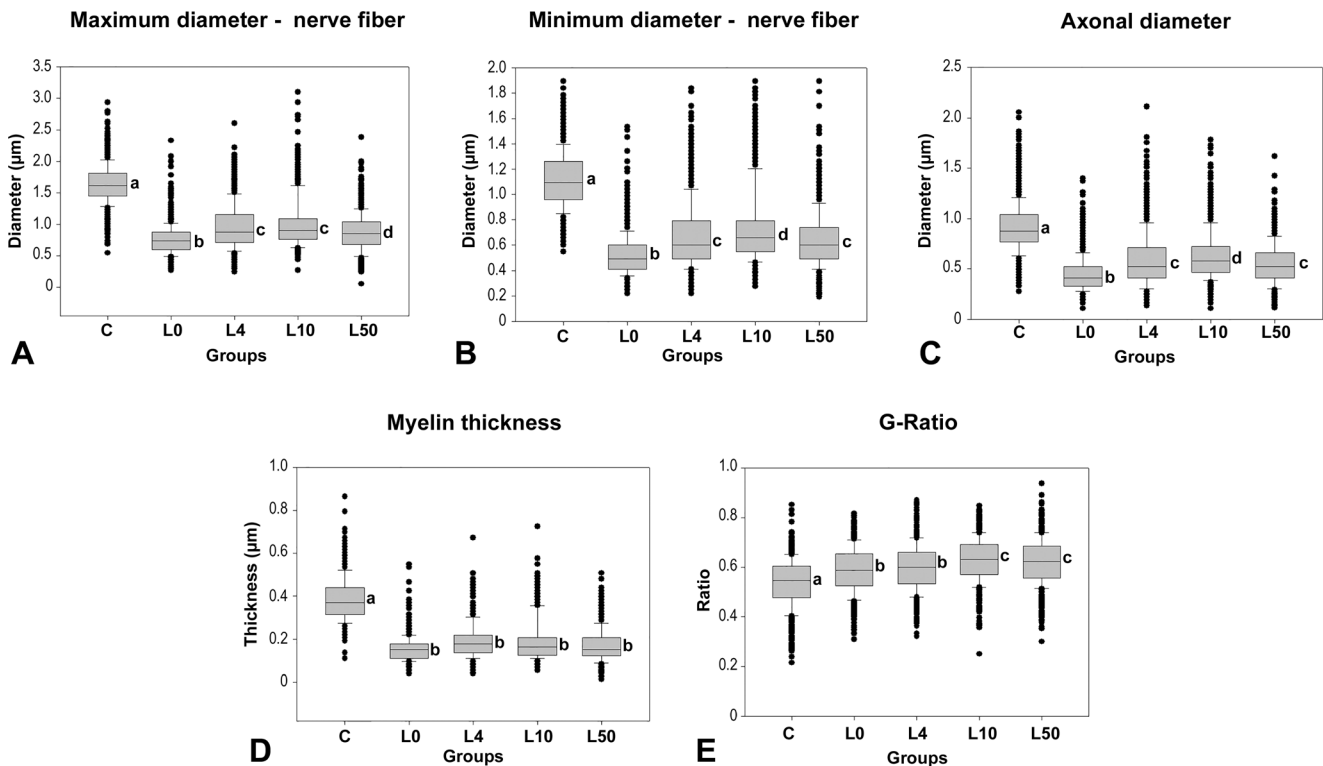
Fig. 4 Morphometric analysis. **a** Morphometric analysis graph of the maximum diameter nerve fibers for the six rats of the study groups; the *letters* represent significant differences ($p < 0.05$). **b** Morphometric analysis graph of the minimum diameter nerve fibers for the six rats of the study groups; the *letters* represent significant differences ($p < 0.05$). **c** Morphometric analysis graph of the axon diameter for the six rats of the study groups, the *letters* represent significant difference ($p < 0.05$). **d** Morphometric analysis graph of the thickness of the myelin sheath for the six rats of the study groups; the *letters* represent significant differences ($p < 0.05$). **e** Morphometric analysis graph of the G-ratio (ratio of axonal diameter/maximum diameter nerve fiber) for the six study groups. In all graphs, the *different letters a*, *b*, *c*, and *d* represent significant differences ($p < 0.05$) among the groups, and the *similar letters* represent no significant differences ($p > 0.05$) among the groups

Discussion

In our study, three low-level laser (LLLT) energy densities were applied after nerve crush injuries to sciatic nerves. The load used for the lesion was 15 kgf (10 min), and the analysis was performed after 15 days; thus, it was possible to assess the effect of LLLT immediately after irradiation protocol. Three LLLT energy densities (4, 10, and 50 J/cm^2) were chosen according to previous literature [12, 14, 16] to assess three energy density levels: low, medium, and high.

The variability of the physical parameters (energy density, wavelength, intensity, power, and irradiation time) of LLLT remains a subject of discussion. In this type of study, it is increasingly important to improve how such variations are managed and to employ the best physical parameters for each case. The variability of the energy density applied to the nerve injury is wider than that proposed in previous studies, which ranged from 1 J/cm^2 [11] to 450 J/mm^2 [29]. However, we evaluated three densities that were frequently used in previous studies [11–18, 30]. The 15-kgf load was chosen for its known ability to induce axonal injury [23].

The morphological analysis showed that the control group with normal characteristics contained many densely distributed nerve fibers in the cross-sectional area that were larger compared to the injured groups (L0, L4, L10, and L50). These observations are consistent with Wood et al. [31], who reported demyelination as a consequence of crush injury to peripheral nerves. The injured and irradiated groups (L4, L10, and L50) revealed better features compared to the L0 group. These groups exhibited more nerve fibers with better distributions and larger sizes, but these features were still below those observed in the control group after 15 days of nerve injury. Among the treated groups, the L10 group presented morphology closest to that of the control group, with a better organization and distribution of nerve fibers. The likely reasons for such improvements include the possibility that the LLLT, due to its photochemical and photobiological effects at the cellular level, may induce trophic conditions and inhibit inflammatory processes, which is necessary for nerve regeneration, thus improving the growth of neurite ATP production, gene expression, and the secretion of neural factors [10, 11]. Data from quantitative analysis decreased after nerve injury. The myelin density revealed no significant differences between the irradiated animals with the injured-only animals. However, a trend of rising values in the treated groups was observed. The capillary density values of the L4 and L50 groups reached values

similar to the control group, and the L10 group showed even greater values than the control. These data are relevant because increased vascular permeability and angiogenesis are crucial for wound healing. The increase in vascular permeability allows cytokines and growth factors to reach the injured tissue [32].

The morphometric analysis corroborates previous analyses. The maximum and minimum diameters of the nerve fibers, the axonal diameter, and the myelin sheath thickness had reduced values in the L0 group. The LLLT (L4, L10, and L50) groups showed higher values than the L0 group, although the treated groups did not reach values similar to the control. The minimum nerve fiber diameter and axon diameter of the L10 group were closer to the control, and the maximum diameter and myelin sheath thickness of the L10 group which was followed by the L4 group were the closest to the control values.

The G-ratio of all of the groups showed values close to the ideal value of 0.6 [26, 33, 34]. However, the nerve injury and irradiation by the LLLT led to increases in the morphometric parameters, and energy densities of 10 to 50 J/cm^2 represented the highest values.

The quantitative and morphometric analysis, even though they are not directly related to functional evaluation (motor and/or sensory), can suggest improvements, since these parameters correlate with the functional outcome of the nerve recovery [35].

Many recent studies have assessed nerve recovery after crush injury using the LLLT. Belchior et al. [12] and Barbosa et al. [14] both used 660-nm wavelength laser with energy densities ranging from 4 to 10 J/cm^2 and reported histopathological and functional improvements in post-injury. Gigo-Benato et al. [15] also used 660-nm LLLT and energy densities of 10 to 60 J/cm^2 and succeeded in restoring muscle fiber-associated pinched nerve and improving the myelin sheath of the nerve and the area of the transverse section. The same energy densities also applied to 780-nm laser, which restored normal levels of myelin and cross-sectional areas of nerve fibers but did not prevent muscular atrophy.

There is indeed a large variation among the physical parameters of LLLT for the treatment of nerve injuries. This study included utilized 780-nm LLLT applied at three different power densities of 4, 10, and 50 J/cm^2. The Twin Laser MMOptics equipment has two wavelengths, 660 and 780 nm, in different probes, the 780-nm wavelength was chosen due to its greater ability to penetrate organic tissues [36] and thus deliver more energy to deeper tissues, such as the sciatic nerve. Gigo-Benato et al. [15] employed the same wavelength and also achieved positive results with similar energy densities. However, the authors mentioned the lack of prevention of muscle atrophy, which was not examined in this study. Moreover, Belchior et al. [12] and Barbosa et al. [14] used 660-nm lasers and obtained positive results with

energy densities of 4 and 10 J/cm^2 in injured nerves, as in the present study.

After sciatic nerve crush, the thickness of the myelin sheath was significantly increased in the animals administered irradiation with 808-nm LBI at 3 and 8 J/cm^2. Treatment at such low energy densities enhances regeneration of crushed peripheral nerve [19]. Takhtfooladi et al. [20] reported improvements in the sciatic functional index (SFI) and the static sciatic index (SSI) after 14 and 21 days of sciatic nerve crush (5.4 kg) treated with LLLT (685 nm, 15 mW, CW, 3 J/cm^2).

These studies [19, 20] disclosed a laser treatment to treat crush injuries that employed moderate (8 J/cm^2) and low (3 J/cm^2) energy density values, in contrast to previous studies that have utilized densities up to 450 J/mm^2 [29]. Our results showed improvements for all densities applied, including densities of 4 to 10 J/cm^2. This finding is in agreement with this latest reports, albeit not tested for energy densities as high as 450 J/mm^2, which suggests an exaggerated energy density according to current standards.

Although several studies have reported favorable results employing LLLT for treatment of nerve injury, other studies have shown no such improvement. Crushed peroneal nerves of rats (5 kgf, 10 min) irradiated with LLLT (830 nm, 30 mV, 10.34 J/cm^2) for 14 consecutive days exhibited no difference compared to injured animals without irradiation. No significant differences were observed regarding the number of Schwann cells, and the number of myelinated nerve fibers was not sufficient for improving neural function. The nerve fibers of the injured groups had a lower diameter, and LLLT showed no positive influence on the recovery of peripheral nerves [30]. Another study regarding crushed peroneal nerves (5 kg/f) considering the application of various energy densities of LLLT (830 nm; 5, 10, and 20 J/cm^2; 21 days) showed no improvements in function (peroneal functional index), nerve cross-sectional area, and nerve fiber density [18]. The animal gait analysis for crushed sciatic nerve and irradiated with different energy densities of 830 nm LLLT showed that 40 and 80 J/cm^2 were more effective, supporting the World Association for Laser Therapy that does not recommend irradiation at densities of 10 J/cm^2 for peripheral nerve compression cases [17].

The negative results observed in studies considering peroneal nerve [18, 30] are likely not due to the use of this nerve. The use of 830-nm LLLT by Marcolino et al. [17] may be related to the negative results, as all other studies utilizing other wavelengths observed at least some positive results.

The recommendation by the World Association for Laser Therapy regarding the use of 10 J/cm^2 would not be indicated for the treatment of crush injuries of peripheral nerves [17]. This fact draws attention that, as in our study, the energy density of 10 J/cm^2 induced the best results following injury. As in several other studies, some discussed here, the use of 10 J/cm^2 or comparable energy density also led to

improvements in nerves post-injury. Therefore, the physical parameters of LLLT must be taken into consideration, which goes far beyond just the chosen energy density, to improve the biological frameworks. In this study, in addition to energy density, we suggest that the type of tissue modification/injury and other parameters, such as the wavelength and type of radiation, must always be considered.

This controversy illustrates the need for additional studies to better understand how the various settings and parameters of low-level lasers affect nerve injury treatments.

Conclusions

In conclusion, the morphological, morphometric, and quantitative results 15 days after sciatic nerve injury due to a load of 15 kgf revealed different outcomes. The 780-nm low-level laser induced improvement in the injury status for various energy densities (4, 10, and 50 J/cm^2), but the improvements did not reach control levels, which showed the best results. However, among the evaluated energy densities, the 10 J/cm^2 was the most effective treatment for improving the post-injury period.

References

1. Lundborg G (1987) Nerve regeneration and repair. A review. Acta orthop scand 58:145–169
2. Evans GR (2001) Peripheral nerve injury: a review and approach to tissue engineered constructs. Anat rec 263:396–404
3. Raimondo S, Fornaro M, Tos P et al (2011) Perspectives in regeneration and tissue engineering of peripheral nerves. Ann anat 193:334–340
4. Martínez De Albornoz P, Delgado PJ, Forriol F, Maffulli N (2011) Non-surgical therapies for peripheral nerve injury. Br med bull 100:73–100
5. Shen CC, Yang YC, Liu BS (2011) Large-area irradiated low-level laser effect in a biodegradable nerve guide conduit on neural regeneration of peripheral nerve injury in rats. Injury 42:803–813
6. Dubový P (2011) Wallerian degeneration and peripheral nerve conditions for both axonal regeneration and neuropathic pain induction. Ann anat 193:267–275
7. Rovak JM, Mungara AK, Aydin MA et al (2004) Effects of vascular endothelial growth factor on nerve regeneration in acellular nerve grafts. J reconstr microsurg 20:53–58
8. Morries LD, Cassano P, Henderson TA (2015) Treatments for traumatic brain injury with emphasis on transcranial near-infrared laser phototherapy. Neuropsychiatr dis treat 11:2159–2175
9. Hashmi JT, Huang YY, Osmani BZ et al (2010) Role of low-level laser therapy in neurorehabilitation. PM R 12:s292–s305
10. Gomes LE, Dalmarco EM, André ES (2012) The brain-derived neurotrophic factor, nerve growth factor, neurotrophin-3, and induced nitric oxide synthase expressions after low-level laser therapy in an axonotmesis experimental model. Photomed laser surg 30:642–647
11. Yazdani SO, Golestaneh AF, Shafiee A et al (2012) Effects of low level laser therapy on proliferation and neurotrophic factor gene expression of human Schwann cells in vitro. J photochem photobiol b 107:9–13
12. Belchior AC, Dos Reis FA, Nicolau RA et al (2009) Influence of laser (660 nm) on functional recovery of the sciatic nerve in rats following crushing lesion. Lasers med sci 24:893–899
13. Dos Reis FA, Belchior AC, De Carvalho PT et al (2009) Effect of laser therapy (660 nm) on recovery of the sciatic nerve in rats after injury through neurotmesis followed by epineural anastomosis. Lasers med sci 24:741–747
14. Barbosa RI, Marcolino AM, De Jesus Guirro RR et al (2010) Comparative effects of wavelengths of low-power laser in regeneration of sciatic nerve in rats following crushing lesion. Lasers med sci 25:423–430
15. Gigo-Benato D, Russo TL, Tanaka EH et al (2010) Effects of 660 and 780 nm low-level laser therapy on neuromuscular recovery after crush injury in rat sciatic nerve. Lasers surg med 42:673–862
16. Medalha CC, Di Gangi GC, Barbosa CB et al (2012) Low-level laser therapy improves repair following complete resection of the sciatic nerve in rats. Lasers med sci 27:629–635
17. Marcolino AM, Barbosa RI, Das Neves LM, Mazzer N, De Jesus Guirro RR, De Cássia Registro Fonseca M (2013) Assessment of functional recovery of sciatic nerve in rats submitted to low-level laser therapy with different fluences. An experimental study: laser in functional recovery in rats. J hand microsurg 5:49–53
18. Sene GA, Souza FF, Fazan VS, E Barbieri CH (2013) Effects of laser therapy in peripheral nerve regeneration. Acta ortop bras 21:266–270
19. Wang CZ, Chen YJ, Wang YH, Yeh ML, Huang MH, Ho ML, Liang JI, Chen CH (2014) Low-level laser irradiation improves functional recovery and nerve regeneration in sciatic nerve crush rat injury model. Plos one 9:e103348
20. Takhtfooladi MA, Jahanbakhsh F, Takhtfooladi HA, Yousefi K, Allahverdi A (2015) Effect of low-level laser therapy (685 nm, 3 J/cm2) on functional recovery of the sciatic nerve in rats following crushing lesion. Lasers med sci 30:1047–1052
21. Dias FJ, Issa JPM, Coutinho-Netto J et al (2015) Morphometric and high resolution scanning electron microscopy analysis of low-level laser therapy and latex protein (*Hevea brasiliensis*) administration following a crush injury of the sciatic nerve in rats. J neurol sci 349:129–137
22. Muniz KL, Dias FJ, Coutinho-Netto J et al (2015) Properties of the tibialis anterior muscle after treatment with laser therapy and natural latex protein following sciatic nerve crush. Muscle nerve 52:869–875

23. Schiaveto De Souza A, Da Silva CA, Del Bel EA (2004) Methodological evaluation to analyze functional recovery after sciatic nerve injury. J neurotrauma 21:627–635

24. Behmer OA, Tolosa EMC, Freitas Neto AG (1976) Manual of techniques for normal and pathological histology [Portuguese] 1 ed. EDART, Editora da Universidade de São Paulo, São Paulo

25. Arino H, Brandt J, Dahlin LB (2008) Implantation of Schwann cells in rat tendon autografts as a model for peripheral nerve repair: long term effects on functional recovery. Scand j plast reconstr surg hand surg 42:281–285

26. Chomiak T, Hu B (2009) What is the optimal value of the g-ratio for myelinated fibers in the rat CNS? A theoretical approach. Plos one 4:e7754

27. Santos AP, Suaid CA, Xavier M, Yamane F (2012) Functional and morphometric differences between the early and delayed use of phototherapy in crushed median nerves of rats. Lasers med sci 27:479–486

28. Holm S (1979) A simple sequentially rejective multiple test procedure. Scand j stat 6:65–70

29. Rochkind S, Leider-Trejo L, Nissan M et al (2007) Efficacy of 780-nm laser phototherapy on peripheral nerve regeneration after neurotube reconstruction procedure (double-blind randomized study). Photomed laser surg 25:137–143

30. Sousa FF, Ribeiro TL, Fazan VP, Barbieri CH (2013) Lack of effectiveness of laser therapy applied to the nerve course and the correspondent medullary roots. Acta ortop bras 21:92–97

31. Wood MD, Kemp SW, Weber C, Borschel GH, Gordon T (2011) Outcome measures of peripheral nerve regeneration. Ann anat 193: 321–333

32. Mendonça RJ, Maurício VB, Teixeira Lde B, Lachat JJ, Coutinho-Netto J (2010) Increased vascular permeability, angiogenesis and wound healing induced by the serum of natural latex of the rubber tree Hevea brasiliensis. Phytother res 24:764–768

33. de Campos D, Heck L, Jotz GP (2014) Degree of myelination (G-ratio) of the human recurrent laryngeal nerve. Eur arch otorhinolaryngol 271:1277–1281

34. Rushton WA (1951) A theory of the effects of fibre size in medullated nerve. J physiol 115:101–122

35. Raimondo S, Fornaro M, Di Scipio F et al (2009) Chapter 5: methods and protocols in peripheral nerve regeneration experimental research: part II-morphological techniques. Int rev neurobiol 87:81–103

36. Byrnes KR, Waynant RW, Ilev IK et al (2005) Light promotes regeneration and functional recovery and alters the immune response after spinal cord injury. Lasers surg med 36:171–185